Dynamic Inversion-Based Control Concept for Transformational Tilt-Wing eVTOLs

Daniel Milz and Marc May and Gertjan Looye

Transformational electric vertical take-off and landing (eVTOL) vehicles, including tiltwings, have (re)gained popularity over the past decade owing to their advantages of efficient wing-borne cruise flight and reduced requirements on ground-based infrastructure. They promise a new mode of transportation for fast and versatile, short-to-medium-haul on-demand connections. However, they come at the cost of complex mechanics, flight dynamics, and aerodynamics. Among these factors, the different flight regimes and the transition between them make the control system design challenging. Ideally, a flight control system provides means for pilot interaction, autoflight functions, robustness to disturbances, and failure mitigation. The different flight regimes with distinct flight dynamics in a single vehicle motivate a holistic approach. So far, no control approach has prevailed, which raises the question of how to design a control concept that satisfies the above requirements for the full flight envelope. To solve this problem, we derive a generalized representation for transformational eVTOLs and propose a flight control approach for this system, consisting of a dynamic-inversion-based angular rate and velocity control law. Moreover, combining these control functions with optimization-based control allocation is motivated and presented. Finally, the concept is applied to a tandem tilt-wing configuration and analyzed. Results suggest the practicability of the proposed control approach.

Dynamic Inversion-Based Control Concept for Transformational Tilt-Wing eVTOLs

Daniel Milz* and Marc May† and Gertjan Looye‡
Institute of System Dynamics and Control, German Aerospace Center (DLR), 82234 Weßling, Germany

Transformational electric vertical take-off and landing (eVTOL) vehicles, including tilt-wings, have (re)gained popularity over the past decade owing to their advantages of efficient wing-borne cruise flight and reduced requirements on ground-based infrastructure. They promise a new mode of transportation for fast and versatile, short-to-medium-haul on-demand connections. However, they come at the cost of complex mechanics, flight dynamics, and aerodynamics. Among these factors, the different flight regimes and the transition between them make the control system design challenging. Ideally, a flight control system provides means for pilot interaction, autoflight functions, robustness to disturbances, and failure mitigation. The different flight regimes with distinct flight dynamics in a single vehicle motivate a holistic approach. So far, no control approach has prevailed, which raises the question of how to design a control concept that satisfies the above requirements for the full flight envelope. To solve this problem, we derive a generalized representation for transformational eVTOLs and propose a flight control approach for this system, consisting of a dynamic-inversion-based angular rate and velocity control law. Moreover, combining these control functions with optimization-based control allocation is motivated and presented. Finally, the concept is applied to a tandem tilt-wing configuration and analyzed. Results suggest the practicability of the proposed control approach.

I. Introduction

Electric Vertical Take-off and Landing (eVTOL) vehicles have the potential to expand the mobility infrastructure to a historic scale. Their ability to take off and land in most terrains and situations opens up new possibilities. Although this is already possible for small unmanned aerial vehicles (SUAVs), vehicles the size of general aviation aircraft and manned operations are only possible with helicopters. However, electric vehicles and distributed electric propulsion open up new ways in this manner and may revive the dream of transformational flight vehicles - hybrids of helicopters and aircraft - with VTOL capability.

In the early days of flight, pioneers already sought a way to make aircraft less dependent on infrastructure, arriving at concepts like autogyros in the 1920s. These developments led to the invention of the first helicopters in the late 1930s. However, these had the major drawback of inefficient flight compared to fixed-wing aircraft. During the 1950s to '70s, various projects aimed at developing transformational vehicles, of which many were tilt-wing or ultimately thrust vectoring vehicles [1]. It was thought to be of military advantage during the Cold War. A famous project during this time was the Canadair CL-84, considered the world's first successful tilt-wing aircraft and gained worldwide attention [2]. The engineers included several means to mitigate the complex dynamics of tilt-wings including a clever arrangement of cams and levers for the same control movements regardless of the wing's position, reducing pilot training (for hover flight), as well as stability augmentation systems in low-speed flight [2]. Despite crashes, the prototypes were a great success, and many flight test hours were accumulated. Although pushed by the US Navy during the Vietnam War, there were no military contracts, and the program ended after the war in the '70s. Other notable projects were carried out by Convair, Dassault Aviation, Dornier, EWR Entwicklungsring Süd, Lockheed, Bell, Rockwell International, LTV, Hiller, Bristol Siddeley, and Hawker Siddeley. In the 1980s, Bell and Boeing started developing the V-22 Osprey as the first operational tilt-rotor aircraft. It combines the vertical take-off and landing capabilities of helicopters with the speed and range of fixed-wing aircraft. Its pre-predecessor, the Bell XV-3, was the first tilt-rotor aircraft to successfully convert from helicopter to fixed-wing mode in 1958 [3]. The transformational aircraft that have been delivered and successfully commissioned are of particular interest. Besides the Osprey, known representatives are military jets of the late 20th and

*Research Associate, Department of Aircraft Systems Dynamics, daniel.milz@dlr.de
†Research Associate, Department of Aircraft Systems Dynamics, marc.may@dlr.de
‡Head of Department, Department of Aircraft Systems Dynamics, gertjan.looye@dlr.de

21st centuries. The most famous include the Hawker Siddeley Harrier, the Jakowlew Yak-38, and today's Lockheed Martin F-35 Lightning II. In the early 2000s, quadcopters began to gain popularity as SUAVs with VTOL capabilities. These were the precursors of personal/on-demand/advanced air vehicles, which attracted much attention in the 2010s and 2020s. These strive for the same advantages as their predecessors: Combining the VTOL and hover capabilities of helicopters with the efficiency, speed, and range of fixed-wing aircraft. Developments in digital, electric motor, and battery technologies make it possible to realize unprecedented configurations with distributed electric propulsion at low cost.

Although former applications were heavily military-driven, current developments aim at advanced air mobility operations for civil manned transport. There, different configurations have emerged. While multicopters are designed for short distances and compete with existing services such as taxis or public transportation, transformational eVTOLs are designed for medium distances and meet the demand for new connections. Transformational eVTOLs include all eVTOLs that alter their "form" during different flight phases encompassing tilt-wing and tilt-rotor aircraft. Thus, transformational vehicles are particularly interesting because they offer infrastructure-independent take-off and landing while providing efficient wing-borne flight. Moreover, from a technological point of view, it is of utmost interest to study transformational vehicles since they can perform maneuvers and missions that are otherwise impossible for conventional aircraft. Although their applications will mainly benefit combat and advanced air mobility, they may also be of interest for search and rescue operations and in rugged terrain and situations. It should also be noted that transformational eVTOLs have a limited field of operational applications. Short-distance connections and operations requiring long hover times are better served by helicopters, multicopters, or even trains and cars. Whereas long-distance connections and connections with suitable infrastructure at the start and end points can be covered more efficiently by fixed-wing aircraft, including STOL configurations. However, in their niche of infrastructure-agnostic, medium-distance, on-demand transportation, transformational eVTOLs have a serious advantage.

In the category of transformational aircraft, tilt-rotors and tilt-wings are the most promising candidates [4]. However, in contrast to tilt-wings, tilt-rotor vehicles require complex propulsion systems and have drawbacks in aerodynamic efficiency [5]. Nevertheless, there are several reasons why tilt-wings have not been adopted to date. The main one is the technological challenge, which includes the battery technology but also the complex mechanics of the tilting mechanism and complex aerodynamics. Additionally, but common to most eVTOL categories, certification issues are still not fully resolved. Furthermore, future eVTOL pilots face high requirements because transformational eVTOLs operate unprecedentedly, combining helicopter and aircraft modes. As a result, pilots have difficulties controlling these vehicles. An example is the three-hand problem of the Harrier jet, where the pilot must simultaneously operate the thrust lever, stick, and nozzle angle lever during take-off and landing [6], or the complex mechanical design of the CL-84, which ultimately led to crashes of the prototype [2]. Last but not least, public acceptance is a crucial point. Several important aspects that need to be met in order for consumers to use eVTOL transportation services have been identified [7]. The main aspect is safety concerns due to the novelty of eVTOLs.

A particularly noteworthy solution to handle the complex dynamics is a unified control scheme, where the pilot has a single clean interface to control all occurring flight modes. This solution evades the need for extensive training. The need for a unified control system, combining different flight modes into a single control interface for the pilot, probably first arose at the UK Royal Aircraft Establishment with the development of the Vector thrust Aircraft Advanced Control (VAAC) for the AV-8B Harrier in the 1970s to 1980s [8]. The VAAC Harrier has attempted to solve the Harrier's three-hand problem. The VAAC Harrier was modified so pilots could operate without special training using a hand-on-throttle-and-stick control principle [9]. The research results were never actually implemented as another Harrier update. However, these results were fundamental to developing the F-35B Lightning II [8]. Interestingly, it took years and a huge team of engineers to make the controls unified and simple. With this solution, it is possible to release the lever and stick while hovering, and the aircraft will stabilize itself.

The aforementioned issues must be addressed to bring tilt-wing and other transformational eVTOLs closer to market.

A. Problem Statement

The context of this research is the development of a transferrable control law for (tandem) tilt-wing aircraft and, ultimately, transformational eVTOLs. In particular, the control system must provide means for pilot interaction, robust flight in the presence of disturbances, and failure mitigation. Pilot interaction is mainly related to the topic of unified control, for instance, applied in [6, 8, 10], while robust control is of particular interest in urban and close-to-ground operations, where gusts and urban canyons pose unique risks. Failure mitigation of these vehicles is, for example, motivated in [11, 12] and of special interest for the transforming element. Furthermore, the different flight regimes with

distinct flight dynamics and the transition between them must be appropriately handled. In most fixed-wing aircraft or helicopters, the structure of the system changes only slightly over the flight envelope, if at all. However, transformational aircraft inherently change the system structure during the transition to different flight regimes. Furthermore, the cascaded control structures originating from the nature of fixed-wing aircraft dynamics, which are valid according to the singular perturbation theorem or the two-scale separation principle [13], are only partly applicable to transformational eVTOLs. This is because transformational vehicles have an additional, structure-changing state that influences the dynamics and has to be considered in the control design. In addition, transformational vehicles are, in most cases, not only controlled by (primarily) moment-generating actuators but also by (primarily) force-generating effectors. So far, no control approach has been established, which raises the question of how to design a control concept that satisfies the above requirements for the full flight envelope. A special focus lies on the application of tilt-wing eVTOLs but also on the transferability to other transformational eVTOL concepts.

B. State-of-the-Art

EVTOLs are currently much-investigated vehicles. However, research groups and researchers focusing on (tandem) tilt-wing configurations or transformational eVTOLs are limited.

Flight Dynamics In [11, 14], several approaches to modeling and simulating the aerodynamic properties of a tilt-wing are shown. Those include the Vortex Particle Method (e.g., DUST), CFD, Doublet/Vortex Lattice Method (e.g., OpenVSP), and semi-empirical approaches (e.g., Strip Theory). Of special interest is the Vortex Particle Method, which was successfully applied to a tilt-wing configuration in [14, 15]. They provide an accurate though computationally affordable solution to (tilt-wing) aerodynamics. However, the complexity is still high due to the nature of the aircraft configurations, which comprise 20 to 30 different dimensions to vary and require large computations [11, 14]. Thus, in the early stages of development, it is more advantageous to employ simpler approaches, such as the semi-empirical strip theory, particularly if the aim is to develop concepts rather than concrete aircraft designs. Additionally, transformational eVTOLs are multidisciplinary vehicles combining multiple dynamics. Particularly, the novel flight mechanical setup needs to be considered. Transforming mechanisms introduce new behavior to the mechanics, including weight and balance changes [16]. Additional disciplines include electric machines, which enable new means of controlling the vehicle due to high bandwidth responses. Those combined with variable blade pitch propellers offer new perspectives but require new modeling approaches to be covered and aligned with the aerodynamic model influenced by those properties. Other relevant publications, which mostly focus on tilt-wings, are [17–21].

Flight Control Lombaerts et al. approached a unified control system for eVTOL vehicles by reviewing the history and discussing the development and evaluation of simplified vehicle operation concepts using simplified models, controls, inceptors, and displays in [6]. The authors say these aspects are "inseparably interconnected" [6]. However, the publication's primary focus is not the inner-loop control system but the outer-loop command modes and envelope limitations. In the publications [22], the authors design an inner-loop control system for an eVTOL vehicle with separate horizontal and vertical propulsion systems. Their approaches use different forms of dynamic-inversion-based control. The control concepts used, nonlinear dynamic inversion (NDI) and incremental nonlinear dynamic inversion (INDI), promise to control a plant in different regimes with different dynamics. They further focus on a unified command framework and describe their findings. A possible structure for a unified control system is introduced. The results are evaluated through current UAM scenarios. In 2016, Di Francesco and Mattei published their work on modeling a tilt-rotor vehicle and developing the corresponding control system based on INDI [23]. The authors conclude that the INDI approach was an "effective way to solve the problem of the dynamic inversion of systems non-affine in the control" [23]. In [24], Yanguo and Huanjin use an eigenstructure assignment algorithm to control a small tilt-rotor aircraft. Hartmann et al. published various findings on tilt-wing aircraft. In [25], the authors attempt to control tilt-wing aircraft via the following control law: A predefined mapping between trim states and control outputs provides the trimmed control output. A disturbance realized via the inversion of a linear control effector matrix gives a mapping between desired forces and moments and control outputs. This disturbance can be used to accelerate or rotate the aircraft. However, this method requires the state to be in a "local attractor's sphere of influence" [25]. Large or fast disturbances thus lead to undetermined and possibly unstable behavior. In [26], the authors show a method for a unified velocity control scheme for tilt-wing aircraft, improving the method from [25]. They introduced virtual control inputs to combine the effect of multiple control inputs. A control allocation scheme is, therefore, needed. The control allocation is a static mapping. Tilting the wing in a "thrust-borne" (vertical) flight or adjusting the body pitch angle in a "wing-borne"

(horizontal) flight changes the effective wing angle [26]. The primary control law uses gain scheduling: The control effectiveness matrix that maps control outputs to forces and moments is inverted. Thus, desired forces and moments can be used to calculate corresponding control outputs. A "set of characteristic maps" [26] stores the inverse of the effectiveness matrix. Another research group published several papers on the construction, aerodynamic analysis, and control design of a novel quad tilt-wing UAV [27, 28]. In [27], they describe the process from the initial design, the model generation and analysis, and the control design to experimental tests. The control system uses virtual control inputs from a high-level controller to a low-level controller scheduled depending on the current tilt angle via a lookup table [28]. The tilt angle follows the required velocity [28].

The studies around [29] are worth mentioning, as they address a generic solution for the control of transition VTOLs. However, they consider a different configuration and assumptions derived from it, as well as choosing a rather complex solution in its entirety.

New developments in transformational or tilt-wing eVTOL control include the application of NDI to a (tandem) tilt-wing UAV in [18, 19, 30]. The control system is divided into a moment-controlling and force-controlling part to enable further uncoupling of motion. The moment-controlling part is expounded upon in [18, 19]. It features an attitude controller, along with a (linear) control allocation strategy that can handle failures and integrates anti-wind-up techniques for saturating actuators. In [19], a universal method for outer-loop velocity control is presented. This approach simplifies the two-dimensional inversion problem (comprising vertical and horizontal velocity) into a one-dimensional problem by commanding a generalized force and tracking a compound velocity. The pitch attitude controller is utilized to stabilize and track the internal dynamics. While the approach is elegant and generic, the controller is tailored to track yaw rates and earth-centered velocities. Although this approach is favored for thrust-borne flight regimes, it is uncommon in wing-borne flight regimes. Another current approach is applying learning-based control methods to a single tilt-wing UAV in order to be controlled [31]. Although the results show promising developments, the technology is still far from being certifiable. In [32], the authors show the development of a tool to tune controller parameters for eVTOLs. However, the work focuses on tuning the linear compensator and does not cover optimizing the nonlinear parts.

In a previous publication, we already published a proof-of-concept unified control law for tandem tilt-wing eVTOLs [10]. There, the focus was on demonstrating the capability of dynamic-inversion-based control approaches to tilt-wings. We, as opposed to [19], tried to invert the angular rate dynamics and the velocity dynamics to achieve thrust and tilt angle commands from the inversion. The thrust distribution was based on a heuristic mapping. It could be shown that this approach can control the tilt-wing, but no statements could be made about the advantages and disadvantages of this approach in comparison to, e.g., [19, 33].

Dynamic inversion, especially incremental NDI, is a practical method to achieve control laws robust to model uncertainties [34]. This is advantageous for transformational vehicles since those often pose complex and nonlinear dynamics - especially their aerodynamics. Due to its substitution of internal dynamics with sensor measurements, incremental NDI is established as a - if not the most - promising control approach for transformational vehicles [10]. However, current applications of dynamic inversion are mostly restricted to fixed-wing aircraft. However, for fixed-wing aircraft, it is established to build control-loop cascades. E.g. [35, 36] uses a body angular rate control loop for (p, q, r), wrapped by an aerodynamic angle control loop for (ϕ, α, β), again wrapped by the navigation control loop for (V, γ, χ). This is a - in its variations - common approach. Other authors use an inner loop for the ϕ, θ, β control and wrap it by a flight path control of V, γ, χ loop. An application of this approach to transformational vehicles is, for example, shown in [19], whereas [10] applies a novel kind of transformational control inverting rotational and translational dynamics, similar to [33].

C. Approach

Current research on tilt-wing and transformational aircraft control focuses on scheduling-based or dynamic inversion-based control laws. In contrast, research on dynamic-inversion-based control laws focuses primarily on fixed-wing aircraft or small UAVs (including quadcopters). Furthermore, there were different approaches to the inversion of the transformational flight dynamics. For example, [18, 19] used NDI to invert the angular rate dynamics while using a separate control for the velocity and tilt angle, which are coupled. In contrast, [10, 22, 33] inverts the rotational as well as the translational dynamics in one.

To solve the abovementioned problem, we will derive a generalized representation of transformational eVTOLs from rigid-body 6-DoF (degrees of freedom) equations of motion. A promising flight control approach for this system, consisting of a dynamic-inversion-based angular rate and velocity control law, is then proposed. Moreover, higher-level control functions are motivated, and optimization-based control allocation is combined with dynamic inversion. The

concept is realized and analyzed on a tandem tilt-wing eVTOL. Dynamic-inversion-based methods are utilized since they offer established means of controlling nonlinear dynamics holistically. We will see that the dynamic inversion and the flight control functions are structurally similar for different configurations and can be designed in combination with a control allocation strategy depending on the actual flight vehicle. In contrast, higher-level control functions focus on the general type of configuration and the missions. Those are, however, not part of this work.

II. Flight Dynamics

Let $x \in \mathbb{R}^{n_x}$ denote the system's state vector, $u \in \mathbb{R}^{n_u}$ the input vector, and $y \in \mathbb{R}^{n_y}$ the output vector. Furthermore, let $f : \mathbb{R}^{n_x} \mapsto \mathbb{R}^{n_x}$ denote the internal dynamic function, $g : \mathbb{R}^{n_x} \times \mathbb{R}^{n_u} \mapsto \mathbb{R}^{n_x}$ the non-affine input function, $G : \mathbb{R}^{n_x} \mapsto \mathbb{R}^{n_x} \times \mathbb{R}^{n_u}$ the affine input function, and $h : \mathbb{R}^{n_x} \times \mathbb{R}^{n_u} \mapsto \mathbb{R}^{n_x}$ the output function. Then, a nonlinear system can be described by

$$\dot{x} = f(x) + g(x, u) \tag{1a}$$
$$= f(x) + G(x)u \tag{1b}$$
$$y = h(x, u) \tag{2}$$

Different types of systems are defined above, i.e., the nonlinear and non-input-affine system (1a) and the nonlinear input-affine system (1b). Most fixed-wing aircraft have a structure similar to (1b), whereas most transformational aircraft are represented by a structure similar to (1a).

A. Fixed-Wing Flight Dynamics

Generic Flight Dynamics Rigid-body aircraft flight dynamics are based on the 6-DOF Newton-Euler equations of motion with the translational states, velocity $\boldsymbol{v}^B$ and position $\boldsymbol{r}^N$, and rotational states, attitude $\boldsymbol{\theta}$ and the angular rates $\boldsymbol{\omega}^B$. The transformation matrices from the body to NED frame is $\mathbb{T}_{\mathrm{NB}}$ and from body to Euler angular velocity $\mathbb{T}_{\Phi\mathrm{B}}$. The resulting state space system is

$$\underbrace{\begin{bmatrix} \dot{\boldsymbol{r}}^N \\ \dot{\boldsymbol{v}}^B \\ \dot{\boldsymbol{\theta}} \\ \dot{\boldsymbol{\omega}}^B \end{bmatrix}}_{\dot{x}} = \underbrace{\begin{bmatrix} \mathbb{T}_{\mathrm{NB}}\, \boldsymbol{v}^B \\ \frac{1}{m}\left[\boldsymbol{f}_{\mathrm{a}}^B(x) + \mathbb{T}_{\mathrm{BN}} \boldsymbol{f}_{\mathrm{g}}^N\left(\boldsymbol{r}_z^N\right)\right] - \boldsymbol{\omega}^B \times \boldsymbol{v}^B \\ \mathbb{T}_{\Phi\mathrm{B}}\, \boldsymbol{\omega}^B \\ \boldsymbol{J}^{-1}\left(\boldsymbol{m}_{\mathrm{a}}^B(x) - \boldsymbol{\omega}^B \times \boldsymbol{J}\boldsymbol{\omega}^B\right) \end{bmatrix}}_{f(x)} + \underbrace{\begin{bmatrix} 0 \\ \frac{1}{m}\left[\boldsymbol{f}_{\mathrm{p}}^B(x, \boldsymbol{t}) + \boldsymbol{f}_{\mathrm{a}}'^B(x, \boldsymbol{\delta}_{\mathrm{A}})\right] \\ 0 \\ \boldsymbol{J}^{-1}\left[\boldsymbol{m}_{\mathrm{p}}^B(x, \boldsymbol{t}) + \boldsymbol{m}_{\mathrm{a}}'^B(x, \boldsymbol{\delta}_{\mathrm{A}})\right] \end{bmatrix}}_{g(x,u)} \tag{3}$$

with the internal aerodynamic forces and moments (i.e. dependent on state and not the input) $\boldsymbol{f}_{\mathrm{a}}^B$ and $\boldsymbol{m}_{\mathrm{a}}^B$, the propulsive forces and moments $\boldsymbol{f}_{\mathrm{p}}^B$ and $\boldsymbol{m}_{\mathrm{p}}^B$ depending on the throttle vector $\boldsymbol{t}$ which is part of the input u, and the external aerodynamic forces and moments, i.e. dependent on the control actuator inputs $\boldsymbol{\delta}_{\mathrm{A}}$, $\boldsymbol{f}_{\mathrm{a}}'^B$ and $\boldsymbol{m}_{\mathrm{a}}'^B$.

Fixed-Wing Aircraft On fixed-wing aircraft, control surface deflections are seen, in most cases, as moment-generating inputs. Although, they induce drag and reduced or additional lift, and sometimes a side force, the total forces generated by control surface deflections are in most cases negligible or not relevant for the control task and are compensated by the controller. Thus, it is common to assume $\boldsymbol{f}_{\mathrm{a}}'^B \approx 0$. However, the control surfaces in most cases allow full control of the aerodynamic moment vector $\boldsymbol{m}_{\mathrm{a}}'^B$. Furthermore, the propulsion system effects are, in most cases, only one dimensional, i.e. $\boldsymbol{f}_{\mathrm{p}}^B = \boldsymbol{n}_{\mathrm{p}} T$ with the thrust direction $\boldsymbol{n}_{\mathrm{p}}$ and the total thrust T.

This constellation allows the control of the aircraft rates $\boldsymbol{\omega}^B$ directly, allowing to control the attitude $\boldsymbol{\theta}$, but only to control the absolute flight path velocity V^K through the engines. The remaining two dimensions of the flight path, which is sought to be controlled, can just controlled indirectly. This motivates the use of the classical paradigm in flight control - cascaded control loops. Those are reinforced by the time scale separation principle, since the inner loop, i.e. attitude control loop, has higher bandwidths than the outer loop, i.e. flight path control loop.

B. Transformational Flight Dynamics

It is hard to generalize transformational flight dynamics since a multitude of different configurations exist. However, this section seeks to cover the most commonly used configuration by a generic representation.Transformational

vehicles are usually distinguished from fixed-wing aircraft in two properties. First, transformational aircraft have a *transformation state* σ, which represents the aircraft's current form. For fast dynamics (e.g., some thrust vectoring jets), the transformation state can be simplified to a direct input. Second, in most cases, transformational aircraft have some form of thrust vectoring, i.e., they have a multidimensional propulsive force and moment vector $\boldsymbol{f}_{\mathrm{p}}^{B}$ and $\boldsymbol{m}_{\mathrm{p}}^{B}$. Although special transformational vehicles, such as amphibian UAVs, do not always possess this property, many currently investigated aircraft do (including a multitude of eVTOL configurations). However, in many cases, this comes at the cost of more complex aerodynamics, mainly through effects including post-stall regions, transitional flight phases, low-speed regimes, configuration changes (such as tilting wings), and aerodynamic interactions [16]. This not only increases the complexity of $\boldsymbol{f}_{a}^{B}$ and $\boldsymbol{m}_{a}^{B}$, which sensor-based control laws as incremental NDI could handle, but also of $\boldsymbol{f}_{a}^{\prime B}$ and $\boldsymbol{m}_{a}^{\prime B}$.

It is assumed in this work that the main difference in control design for those transformational vehicles lies in the control allocation and the rank of the input forces and moments. There, higher level force and moment commands are required to be realized by the vehicle. For this, *Actuators* and *Effectors* can be utilized. Actuators are similar to fixed-wing actuators and represent aerodynamic controls. Those heavily depend on the current state - especially the aerodynamic state. They often have high bandwidths and mainly influence the aircraft's moments. Effectors, however, represent the remaining means of control and are mostly engines. With distributed electric propulsion, an aircraft can be equipped with several effectors. Those regularly have lower to medium bandwidths. However, electric propulsion pushes those to the mid to higher bandwidth regions.

Actuators and effectors are represented by an effector "deflection" $\boldsymbol{\delta}_{\mathrm{E}}$ and an actuator "deflection" $\boldsymbol{\delta}_{\mathrm{A}}$. Thus, the relevant dynamics of transformational aircraft can be essentially described by

$$\dot{\boldsymbol{v}}^{B} = \frac{1}{m}\boldsymbol{f}_{\mathrm{a}}^{B}(x) - \boldsymbol{\omega}^{B} \times \boldsymbol{v}^{B} + \frac{1}{m}\left(\boldsymbol{f}_{p}^{B}(x, \boldsymbol{\delta}_{\mathrm{E}}) + \boldsymbol{f}_{a}^{\prime B}(x, \boldsymbol{\delta}_{\mathrm{E}}, \delta_{A})\right) \tag{4}$$

$$\dot{\boldsymbol{\omega}}^{B} = \boldsymbol{J}^{-1}\left(\boldsymbol{m}_{\mathrm{a}}(x) - \boldsymbol{\omega}^{B} \times \boldsymbol{J}\boldsymbol{\omega}^{B}\right) + \boldsymbol{J}^{-1}\left(\boldsymbol{m}_{p}^{B}(x, \boldsymbol{\delta}_{\mathrm{E}}) + \boldsymbol{m}_{a}^{\prime B}(x, \boldsymbol{\delta}_{\mathrm{E}}, \delta_{A})\right) \tag{5}$$

with the state vector x.

In many publications, including [10, 26, 33], the authors assume the transformation state σ to be a (sole) input. However, the transformation is conceptually better represented as a system state and can be represented, in most cases, by low-pass dynamics. Thus, the complete equations of motion of transformational eVTOLs are

$$\underbrace{\begin{bmatrix} \dot{\boldsymbol{r}}^{N} \\ \dot{\boldsymbol{\theta}} \\ \dot{\boldsymbol{v}}^{B} \\ \dot{\boldsymbol{\omega}}^{B} \\ \dot{\boldsymbol{\sigma}} \end{bmatrix}}_{\dot{x}} = \underbrace{\begin{bmatrix} \mathbb{T}_{NB}(\theta)\, \boldsymbol{v}^{B} \\ \mathbb{T}_{\Phi B}(\theta)\, \boldsymbol{\omega}^{B} \\ \frac{1}{m}\boldsymbol{f}^{B}(x) - \boldsymbol{\omega}^{B} \times \boldsymbol{v}^{B} \\ \boldsymbol{J}^{-1}\left(\boldsymbol{m}^{B}(x) - \boldsymbol{\omega} \times \boldsymbol{J}\boldsymbol{\omega}\right) \\ f_{\sigma}(x) \end{bmatrix}}_{f(x)} + \underbrace{\begin{bmatrix} 0 \\ 0 \\ \frac{1}{m}\left(\boldsymbol{f}_{E}^{B}(x, \boldsymbol{\delta}_{\mathrm{E}}) + \boldsymbol{f}_{A}^{B}(x, \delta_{A}) + \boldsymbol{f}_{\mathrm{interact}}^{B}(x, \delta_{A}, \boldsymbol{\delta}_{\mathrm{E}})\right) \\ \boldsymbol{J}^{-1}\left(\boldsymbol{m}_{E}^{B}(x, \boldsymbol{\delta}_{\mathrm{E}}) + \boldsymbol{m}_{A}^{B}(x, \delta_{A}) + \boldsymbol{m}_{\mathrm{interact}}^{B}(x, \delta_{A}, \boldsymbol{\delta}_{\mathrm{E}})\right) \\ g_{\sigma}(x, u) \end{bmatrix}}_{g(x,u)} \tag{6}$$

with the actuator effects having subscript A, effector effects E and interaction terms interact. The interaction terms are required since multiple interactions between actuators and effectors, mainly due to aerodynamic interactions, occur [14]. Additionally, this analysis assumes that actuator and effector dynamics are negligible, making them pure inputs. However, certain configurations may require the consideration of these dynamics.

III. Flight Control Design for Transformational eVTOLs

Although there are plenty of approaches to controlling transformational vehicles, this paper focuses on dynamic inversion-based control approaches.

A. Transformational Flight Control Design

Transformational eVTOLs differ significantly from fixed-wing aircraft as they undergo various flight phases and change their "form." Typically, these phases include hover, transition, and cruise flight. Consequently, a control system must adjust to the changing conditions. Unlike fixed-wing controllers that also make adjustments during flight in the form of scheduling over dynamic pressure, speed, altitude, etc., eVTOL controllers must account for the unique phases of

flight. During flight, they alter the overall system structure: While thrust is the primary control source during hovering, control surfaces become more significant during cruise flight.

Uncoupling the different axes is a beneficial approach. In fact, implementing inversion-based control methods to decouple the control input axes from the outputs reduces the complexity of vehicle control. Inversion enables the calculation of necessary inputs in any transformation state to achieve a desired output in the form of (angular) accelerations. However, as most transformational eVTOLs are overactuated, meaning they are equipped with more control input channels than commanded output channels, implementing control allocation strategies is necessary. Fortunately, dynamic inversion and control allocation pair well together. As (6) suggests, inverting rotational and translational accelerations enables a low relative degree, potentially 1, and thus a direct inversion. The choice is, however, in which form the inversion takes place, especially for the translational acceleration: (6) suggests a direct relation to the acceleration in body frame $\dot{\boldsymbol{v}}^B$, which can also be converted into flight path-centered coordinates (i.e., flight path velocity V^K, flight path angle γ, and course χ), or earth-centered accelerations $\dot{\boldsymbol{v}}^E$. Although most approaches use the body frame as a reference, using a flight path reference system seems to be an alternative solution, as inferred later.

Although the structure of the attitude and velocity controller remains relatively independent of the specific vehicle, the inversion and control allocation must be tailored to the specific vehicle. By contrast, outer-loop control functions, such as the pilot command filter for interfacing with pilot controls or autoflight functions, only require minor adjustments to the specific vehicle in terms of available degrees of freedom and envelope limits but rely on the particular missions and scenarios. For airway-centered missions, controlling the heading and altitude, or their corresponding derivatives, is more beneficial. However, in uncontrolled airspace and free flight, controlling the roll angle and pitch or flight path angle, or their corresponding derivatives, may be desired. The ideal control system would offer both options, but as discussed in e.g. [6], even then, there are still multiple options for the control objective. As a result, the controller can be divided into two parts: a *vehicle-specific* part that includes the inner control loops and a *mission-specific* part that includes the outer control loops. Figure 1 shows the proposed approach to transformational eVTOL control design followed in this publication. This design can be transferred to all transformational eVTOLs fulfilling (6), albeit adjustments in the dynamic inversion and control allocation part.

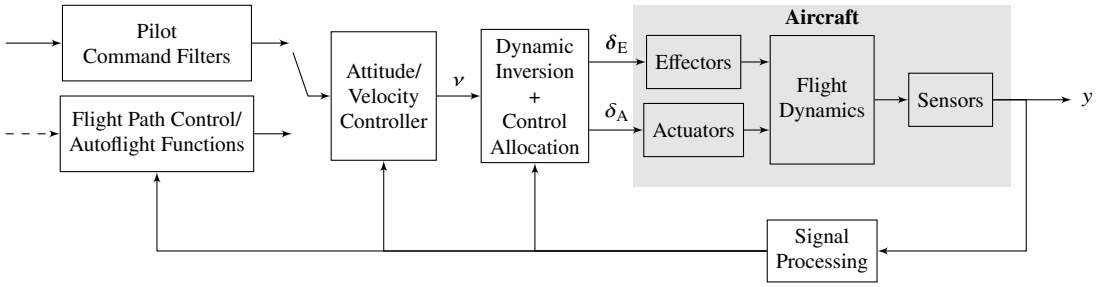

Fig. 1 Generic structure of a controller architecture for transformational eVTOLs.

B. Dynamic Inversion

Assuming a nonlinear system as in (1a), dynamic inversion-based control methods seek to realize a virtual control input ν, which corresponds to the state derivative $\dot{x}$. Nonlinear Dynamic Inversion (NDI) [37] requires an estimation of the state vector $\hat{x}$, and the full system dynamics - i.e. $f(x)$ and $g(x,u)$. With them, the virtual control input can be realized via the implicit control law

$$g(\hat{x}, u_{\text{com}}) = \nu - f(\hat{x}) \tag{7}$$

which can be approximated in the neighborhood of u_0 by

$$\nabla_u g(\hat{x}, u_0)\, u_{\text{com}} \approx \nu - f(\hat{x}) - g(\hat{x}, u_0) + \nabla_u g(\hat{x}, u_0)\, u_0 \tag{8}$$

Sensory NDI [10, 38, 39], but incremental NDI as well, replace the dependency on the internal dynamics $f(x)$ through the sensor measurements $\hat{\dot{x}}$ and $\hat{u}$, yielding the implicit control law

$$g(\hat{x}, u_{\text{com}}) = \nu - \hat{\dot{x}} + g(\hat{x}, \hat{u}) \tag{9}$$

which again can be approximated in the neighborhood of u_0 by

$$\nabla_u g(\hat{x}, u_0)\; u_{\text{com}} \approx \nu - \dot{\hat{x}} + g(\hat{x}, \hat{u}) - g(\hat{x}, u_0) + \nabla_u g(\hat{x}, u_0)\; u_0 \tag{10}$$

and reduces to the control-affine sensory NDI control law, as stated in [10], for an invertible $\nabla_u g(\hat{x}, \hat{u})$ and $u_0 = \hat{u}$ as

$$u_{\text{com}} \approx \; \nabla_u g(\hat{x}, \hat{u})^{-1} \left(\nu - \dot{\hat{x}} + \nabla_u g(\hat{x}, \hat{u})\hat{u}\right) = \hat{u} + \; \nabla_u g(\hat{x}, \hat{u})^{-1} \left(\nu - \dot{\hat{x}}\right) \tag{11}$$

As already shown, the inversion approach depends on the form of the system, and on the knowledge of - at least - the input dynamics. Ideally, the inversion and the control allocation can be split in order to develop both functions independently. However, this requires at least an explicit representation of the system.

With sensory NDI, we can reduce the relevant dynamics form (6) according to (9), yielding

$$\underbrace{\boldsymbol{J}(\nu_\omega - \dot{\hat{\boldsymbol{\omega}}}) + \boldsymbol{m}_u(\hat{\boldsymbol{x}}, \hat{\boldsymbol{u}})}_{\tau_\omega} = \boldsymbol{m}_u(\hat{\boldsymbol{x}}, \boldsymbol{u}_{\text{com}}) \tag{12a}$$

$$\underbrace{m(\nu_v - \dot{\hat{\boldsymbol{v}}}) + \boldsymbol{f}_u(\hat{\boldsymbol{x}}, \hat{\boldsymbol{u}})}_{\tau_v} = \boldsymbol{f}_u(\hat{\boldsymbol{x}}, \boldsymbol{u}_{\text{com}}) \tag{12b}$$

with the combined input moments $\boldsymbol{m}_u = \boldsymbol{m}_E^B(x, \boldsymbol{\delta}_{\text{E}}) + \boldsymbol{m}_A^B(x, \boldsymbol{\delta}_{\text{A}}) + \boldsymbol{m}_{\text{interact}}^B(x, \boldsymbol{\delta}_{\text{A}}, \boldsymbol{\delta}_{\text{E}})$ and input forces $\boldsymbol{f}_u = \boldsymbol{f}_E^B(x, \boldsymbol{\delta}_{\text{E}}) + \boldsymbol{f}_A^B(x, \delta_A) + \boldsymbol{f}_{\text{interact}}^B(x, \delta_A, \boldsymbol{\delta}_{\text{E}})$. Thus, the dynamic inversion objective is to solve (12) for $\boldsymbol{u}_{\text{com}}$. The inverse function theorem, and, finally, the implicit function theorem, give information about the (local) solvability of these types of equations: if the stacked Jacobi matrix

$$\begin{bmatrix} \nabla_u \boldsymbol{m}_u(\hat{\boldsymbol{x}}, \boldsymbol{u}_0) \\ \nabla_u \boldsymbol{f}_u(\hat{\boldsymbol{x}}, \boldsymbol{u}_0) \end{bmatrix} \tag{13}$$

is invertible, then there exists a $\mathcal{K}(\boldsymbol{\nu}, \hat{\boldsymbol{u}}, \hat{\boldsymbol{x}}, \dot{\hat{\boldsymbol{x}}}, \boldsymbol{u}_0) = u_{\text{com}}$ on an open set around $\boldsymbol{u}_0$. It thus allows us to control not only $\boldsymbol{\omega}^B$ in the inner loop but also $\boldsymbol{v}^B$ directly, depending on the rank of the above Jacobian. Furthermore, it is possible to determine which axes or subspaces of $\boldsymbol{\omega}^B$ and $\boldsymbol{v}^B$ cannot and can be controlled directly with the input.

Consequently, this leads to the following sensory NDI control law:

$$\underbrace{\overbrace{\begin{bmatrix} \boldsymbol{J} & \boldsymbol{0} \\ \boldsymbol{0} & m\boldsymbol{I} \end{bmatrix}}^{\boldsymbol{E}} \overbrace{\left(\begin{bmatrix} \nu_\omega \\ \nu_v \end{bmatrix}}^{\boldsymbol{\nu}} - \overbrace{\begin{bmatrix} \dot{\hat{\boldsymbol{\omega}}} \\ \dot{\hat{\boldsymbol{v}}} \end{bmatrix}}^{\dot{\hat{\boldsymbol{x}}}}\right) + \overbrace{\begin{bmatrix} \boldsymbol{m}_u(\hat{\boldsymbol{x}}, \hat{\boldsymbol{u}}) \\ \boldsymbol{f}_u(\hat{\boldsymbol{x}}, \hat{\boldsymbol{u}}) \end{bmatrix}}^{\boldsymbol{g}(\hat{\boldsymbol{x}}, \hat{\boldsymbol{u}})}}_{\tau_0} = \overbrace{\begin{bmatrix} \boldsymbol{m}_u(\hat{\boldsymbol{x}}, \boldsymbol{u}_{\text{com}}) \\ \boldsymbol{f}_u(\hat{\boldsymbol{x}}, \boldsymbol{u}_{\text{com}}) \end{bmatrix}}^{\boldsymbol{g}(\hat{\boldsymbol{x}}, \boldsymbol{u})} \tag{14}$$

where $\boldsymbol{E}$ can be embedded into $\boldsymbol{g}$ directly so that it outputs accelerations instead of forces and moments. The sensory NDI law can be solved explicitly in a neighborhood of $\boldsymbol{u}_0$ through a Taylor series expansion of $\boldsymbol{g}(\hat{\boldsymbol{x}}, \boldsymbol{u})$ as shown in (10).

C. Control allocation

Dynamic Inversion is a generic method that allows for the handling of fixed-wing as well as transformational aircraft in a concise manner. The idea of NDI is to invert the system dynamics in order to get an output vector $\boldsymbol{u}$ based on the estimated current state $\hat{\boldsymbol{x}}$ and the desired (virtual control) output $\boldsymbol{\nu}$. However, we know from the inverse function theorem that we ultimately need $\dim \boldsymbol{u} = \dim \boldsymbol{\nu}$ to be fully and uniquely invertible (assuming the dynamics only have the trivial kernel). This is, in general, not the case. For fixed-wing aircraft, where $\dim \boldsymbol{\nu} = 3$, ganging is commonly used to assign corresponding aileron, elevator, and rudder deflections. New trends in aircraft design bring up more and more control actuators. This is also the case for most transformational aircraft. For instance, the tandem tilt-wing configuration investigated later in this paper has a total of 14 control inputs while $\dim \boldsymbol{\nu} = 5$. Consequently, a scheme is required to assign the remaining control inputs: control allocation. If, through the inversion, the control input is fully determined, control allocation can be skipped. In the case of an over-determined system, i.e., fewer control inputs than commanded degrees of freedom, other approaches are required, which in most cases involve a reduction of the commanded degrees of freedom. It is self-evident that the control allocation has to be tailored to every aircraft configuration in order to achieve the desired results and performance. Related works on transformational eVTOLs follow similar approaches [17, 19, 22, 30, 33, 40].

In order to solve an over-actuated (under-determined) control allocation problem, it is common to introduce an optimization objective $L(\boldsymbol{x}, \boldsymbol{u})$ in addition to the allocation constraint. Consequently, this yields

$$\min_{\boldsymbol{u}} \quad L(\boldsymbol{x}, \boldsymbol{u}) \tag{15a}$$

$$\text{s.t.} \quad \boldsymbol{m}_u(\hat{\boldsymbol{x}}, \boldsymbol{u}) = \boldsymbol{\tau}_\omega \tag{15b}$$

$$\boldsymbol{f}_u(\hat{\boldsymbol{x}}, \boldsymbol{u}) = \boldsymbol{\tau}_\nu \tag{15c}$$

according to (12). For sensory NDI, this depends on the knowledge of the vehicle's input dynamics $\boldsymbol{g}(\boldsymbol{x}, \boldsymbol{u})$ function. An overview of control allocation approaches is given, e.g., in [41, 42]. A promising approach to solve the control allocation problem in combination with dynamic inversion is shown in [34, 40], as well as in the subsequent section.

D. Control allocation and sensory dynamic inversion

Reducing the above-discussed system (14) yields

$$\boldsymbol{g}\left(\hat{\boldsymbol{x}}, \boldsymbol{u}\right) = \underbrace{\boldsymbol{\nu} - \dot{\hat{\boldsymbol{x}}} + \boldsymbol{g}\left(\hat{\boldsymbol{x}}, \hat{\boldsymbol{u}}\right)}_{\boldsymbol{\tau}_0} \tag{16}$$

which can either be solved by iterative solvers or estimated in the linear domain by using the first-order Taylor series expansion of $\boldsymbol{g}$ in the neighborhood of $\boldsymbol{u}_0$ as suggested above

$$\boldsymbol{g}\left(\hat{\boldsymbol{x}}, \boldsymbol{u}\right) = \boldsymbol{g}\left(\hat{\boldsymbol{x}}, \boldsymbol{u}_0\right) + \nabla_u \boldsymbol{g}\left(\hat{\boldsymbol{x}}, \boldsymbol{u}_0\right)\left(\boldsymbol{u} - \boldsymbol{u}_0\right) + O((\boldsymbol{u} - \boldsymbol{u}_0)^2) \tag{17}$$

This allows approaching the nonlinear dynamic-inversion constraint (16) in a linear manner around $\boldsymbol{u}_0$ as

$$\underbrace{\nabla_u \boldsymbol{g}\left(\hat{\boldsymbol{x}}, \boldsymbol{u}_0\right)}_{\boldsymbol{B}} \boldsymbol{u} = \underbrace{\boldsymbol{\nu} - \dot{\boldsymbol{x}} + \boldsymbol{g}\left(\hat{\boldsymbol{x}}, \hat{\boldsymbol{u}}\right) - \boldsymbol{g}\left(\hat{\boldsymbol{x}}, \boldsymbol{u}_0\right) + \nabla_u \boldsymbol{g}\left(\hat{\boldsymbol{x}}, \boldsymbol{u}_0\right) \boldsymbol{u}_0}_{\boldsymbol{\tau}} - O((\boldsymbol{u} - \boldsymbol{u}_0)^2) \tag{18}$$

If $\dim \boldsymbol{u} > \dim \boldsymbol{\tau}$, control allocation methods need to be utilized since the solutions of (16) lie in an at most $(\dim \boldsymbol{u} - \dim \boldsymbol{\nu})$-dimensional subspace of $\mathcal{U}$. Thus, it makes sense to combine the dynamic inversion constraints with the minimization of a cost function $L(\hat{\boldsymbol{x}}, \boldsymbol{u})$. Assuming that L is differentiable twice, and can be approximated by a second-order Taylor series expansion sufficiently (i.e. $O((\boldsymbol{u} - \boldsymbol{u}_0)^3)$ is negligible)

$$L(\hat{\boldsymbol{x}}, \boldsymbol{u}) = L(\hat{\boldsymbol{x}}, \boldsymbol{u}_0) + \nabla_u L(\hat{\boldsymbol{x}}, \boldsymbol{u}_0)\left(\boldsymbol{u} - \boldsymbol{u}_0\right) + \frac{1}{2}\left(\boldsymbol{u} - \boldsymbol{u}_0\right)^T \nabla_{uu} L(\hat{\boldsymbol{x}}, \boldsymbol{u}_0)\left(\boldsymbol{u} - \boldsymbol{u}_0\right) + O((\boldsymbol{u} - \boldsymbol{u}_0)^3) \tag{19}$$

This leads to the following convex optimization problem valid in the neighborhood of $\boldsymbol{u}_0$

$$\begin{aligned} \min_{\boldsymbol{u} \in \mathcal{U}} \quad & L(\hat{\boldsymbol{x}}, \boldsymbol{u}_0) + \nabla_u L(\hat{\boldsymbol{x}}, \boldsymbol{u}_0)\left(\boldsymbol{u} - \boldsymbol{u}_0\right) + \frac{1}{2}\left(\boldsymbol{u} - \boldsymbol{u}_0\right)^T \nabla_{uu} L(\hat{\boldsymbol{x}}, \boldsymbol{u}_0)\left(\boldsymbol{u} - \boldsymbol{u}_0\right) \\ \text{s.t.} \quad & \boldsymbol{B}\boldsymbol{u} = \boldsymbol{\tau} \end{aligned} \tag{20}$$

The optimization problem can be rewritten in Lagrangian form with the Lagrange multiplier $\boldsymbol{\lambda}$ as

$$\mathcal{L} = L(\hat{\boldsymbol{x}}, \boldsymbol{u}_0) + \nabla_u L(\hat{\boldsymbol{x}}, \boldsymbol{u}_0)^T\left(\boldsymbol{u} - \boldsymbol{u}_0\right) + \frac{1}{2}\left(\boldsymbol{u} - \boldsymbol{u}_0\right)^T \nabla_{uu} L(\hat{\boldsymbol{x}}, \boldsymbol{u}_0)\left(\boldsymbol{u} - \boldsymbol{u}_0\right) + \boldsymbol{\lambda}^T\left(\boldsymbol{\tau} - \boldsymbol{B}\boldsymbol{u}\right) \tag{21}$$

where the following optimality conditions denoted in Hessian formulation must hold

$$\frac{\partial \mathcal{L}}{\partial \boldsymbol{u}} = \nabla_u L(\hat{\boldsymbol{x}}, \boldsymbol{u}_0) + \nabla_{uu} L(\hat{\boldsymbol{x}}, \boldsymbol{u}_0)\boldsymbol{u} - \nabla_{uu} L(\hat{\boldsymbol{x}}, \boldsymbol{u}_0)\boldsymbol{u}_0 - \boldsymbol{B}^T\boldsymbol{\lambda} = \boldsymbol{0} \tag{22a}$$

$$\frac{\partial \mathcal{L}}{\partial \boldsymbol{\lambda}} = \boldsymbol{\tau} - \boldsymbol{B}\boldsymbol{u} = \boldsymbol{0} \tag{22b}$$

Consequently, (22a) can be solved for $\boldsymbol{u}$,

$$\boldsymbol{u} = \boldsymbol{u}_0 + \nabla_{uu} L(\hat{\boldsymbol{x}}, \boldsymbol{u}_0)^{-1}\left(\boldsymbol{B}^T\boldsymbol{\lambda} - \nabla_u L(\hat{\boldsymbol{x}}, \boldsymbol{u}_0)\right) \tag{23}$$

Using this expression and (22b) yields

$$\boldsymbol{\lambda} = \left(\boldsymbol{B}\ \nabla_{uu} L(\hat{\boldsymbol{x}}, \boldsymbol{u}_0)^{-1} \boldsymbol{B}^T\right)^{-1} \left(\boldsymbol{\tau} - \boldsymbol{B}\boldsymbol{u}_0 + \boldsymbol{B}\ \nabla_{uu} L(\hat{\boldsymbol{x}}, \boldsymbol{u}_0)^{-1} \nabla_u L(\hat{\boldsymbol{x}}, \boldsymbol{u}_0)\right) \tag{24}$$

which in combination with (23) finally leads to

$$\boldsymbol{u} = \boldsymbol{B}^+ \boldsymbol{\tau} + \left(\boldsymbol{I} - \boldsymbol{B}^+ \boldsymbol{B}\right) \left(\boldsymbol{u}_0 - \nabla_{uu} L(\hat{\boldsymbol{x}}, \boldsymbol{u}_0)^{-1} \nabla_u L(\hat{\boldsymbol{x}}, \boldsymbol{u}_0)\right) \tag{25}$$

with the weighted pseudo-inverse $\boldsymbol{B}^+ = \nabla_{uu} L(\hat{\boldsymbol{x}}, \boldsymbol{u}_0)^{-1} \boldsymbol{B}^T \left(\boldsymbol{B} \nabla_{uu} L(\hat{\boldsymbol{x}}, \boldsymbol{u}_0)^{-1} \boldsymbol{B}^T\right)^{-1}$. In the case of $\nabla_{uu} L(\hat{\boldsymbol{x}}, \boldsymbol{u}_0) = \boldsymbol{I}$, $\boldsymbol{B}^+$ becomes the Moore-Penrose pseudo-inverse. As shown in e.g. [34, 41], (25) can be decomposed into two parts:

- $\boldsymbol{u}^{\parallel} = \boldsymbol{B}^+ \boldsymbol{\tau}$ relates to the inversion constraint (primary goal)
- $\boldsymbol{u}^{\perp} = \left(\boldsymbol{I} - \boldsymbol{B}^+ \boldsymbol{B}\right) \left(\boldsymbol{u}_0 - \nabla_{uu} L(\hat{\boldsymbol{x}}, \boldsymbol{u}_0)^{-1} \nabla_u L(\hat{\boldsymbol{x}}, \boldsymbol{u}_0)\right)$ relates to the optimization objective (secondary goal)

Note that $\boldsymbol{u}^{\perp}$ lies in the null space of $\boldsymbol{B}$, i.e., $\boldsymbol{u}^{\perp} \in \ker \boldsymbol{B}$ and therefore does not affect the inversion (or tracking) constraint but solely the optimization objective. This can be shown through the identity $\boldsymbol{B}\left(\boldsymbol{I} - \boldsymbol{B}^+ \boldsymbol{B}\right) = \boldsymbol{0}$. Furthermore, the dependency of $\boldsymbol{B}^+$ on $\nabla_{uu} L(\hat{\boldsymbol{x}}, \boldsymbol{u}_0)$ does also not influence tracking performance, but distributes $\boldsymbol{u}^{\parallel}$ already accordingly. This can be shown through the identity $\boldsymbol{B}\left(\boldsymbol{B}^+ - \boldsymbol{B}^T \left(\boldsymbol{B}\boldsymbol{B}^T\right)^{-1}\right) = \boldsymbol{0}$ under nominal circumstances. In order to avoid singularities in $\boldsymbol{B}^+$, e.g. due to rank deficiencies of $\boldsymbol{B}$, regularization methods can be utilized [42]. A commonly used method is to utilize the singular value decomposition of $\boldsymbol{B} \nabla_{uu} L(\hat{\boldsymbol{x}}, \boldsymbol{u}_0)^{-1} \boldsymbol{B}^T = \boldsymbol{U}\boldsymbol{\Sigma}\boldsymbol{V}^T$, where $\boldsymbol{\Sigma} = \operatorname{diag}(\sigma_1, \sigma_2, \ldots, \sigma_n)$ contains the singular values. By inverting only non-zero singular values, i.e. $\sigma_i > \epsilon$ with a sufficiently small ϵ, the reduced rank approximation of $\boldsymbol{\Sigma}^{-1}$ is

$$\boldsymbol{\Sigma}^{-1,s} = \operatorname{diag}\left(\frac{1}{\sigma_1}, \ldots, \frac{1}{\sigma_i}, 0, \ldots, 0\right) \tag{26}$$

This leads to a stabilized approximation of the pseudo-inverse

$$\boldsymbol{B}^{+,s} = \nabla_{uu} L(\hat{\boldsymbol{x}}, \boldsymbol{u}_0)^{-1} \boldsymbol{B}^T \boldsymbol{V} \boldsymbol{\Sigma}^{-1,s} \boldsymbol{U}^T \tag{27}$$

Consequently, $\boldsymbol{B}^{+,s}\boldsymbol{\tau}$ solves (16) by using a first-order Taylor series approximation of $\boldsymbol{g}$ in the neighborhood of $\boldsymbol{u}_0$. Additionally, secondary control objectives can be achieved by solving the constraint optimization problem (20). The nonlinear objective is approximated by a second-order Taylor series approximation and its main effect on the control input $\boldsymbol{u}$ is given by $\boldsymbol{u}^{\perp}$ which lies in the null space of $\boldsymbol{B}$. Consequently, it is possible to design $\boldsymbol{u}^{\perp}$ freely in order to achieve objectives on $\boldsymbol{u}$ without degrading the tracking performance as long as $\boldsymbol{u}^{\perp} \in \ker \boldsymbol{B}$. The linear approach to allocate $\boldsymbol{B}\boldsymbol{u} = \boldsymbol{\tau}$ is, however, limited in terms of tracking accuracy. The solution is only valid in the close neighborhood of $\boldsymbol{u}_0$, which is nonlinear for eVTOLs but approximated via a linear hyperplane. In order to increase the accuracy, it may be helpful to substitute the control variables. One may substitute the propeller speed n_i by n_i^2 in order to cover the mainly quadratic influence of the propeller speed on the thrust (and torque). Additionally, the use of ganging [42] as a heuristic pre-allocation reduces the control allocation problem without harming the tracking performance. However, the allocation optimality may be reduced this way. Alternatively, iterative optimization solvers, including interior point methods or SQP, can be utilized to solve the full nonlinear control allocation problem

$$\min_{u \in \mathcal{U}} L\left(\hat{\boldsymbol{x}}, \boldsymbol{u}\right) \tag{28a}$$

$$\text{s.t. } \boldsymbol{g}\left(\hat{\boldsymbol{x}}, \boldsymbol{u}\right) = \boldsymbol{\nu} - \hat{\dot{\boldsymbol{x}}} + \boldsymbol{g}\left(\hat{\boldsymbol{x}}, \hat{\boldsymbol{u}}\right) \tag{28b}$$

This method, however, drastically increases the time to solve the control allocation problem and may fail to find a suitable solution. For complex systems like eVTOLs, it may also be advantageous to solve the multi-objective control allocation problem, ensuring several criteria are met simultaneously and independently,

$$\min_{u \in \mathcal{U}} \max_i \boldsymbol{L}_i\left(\hat{\boldsymbol{x}}, \boldsymbol{u}\right) \tag{29a}$$

$$\text{s.t. } \boldsymbol{g}\left(\hat{\boldsymbol{x}}, \boldsymbol{u}\right) = \boldsymbol{\nu} - \hat{\dot{\boldsymbol{x}}} + \boldsymbol{g}\left(\hat{\boldsymbol{x}}, \hat{\boldsymbol{u}}\right) \tag{29b}$$

However, this method will most likely be used solely offline in order to simulate maneuvers or optimize them (see [12] for related work).

IV. Flight Control Design for a Tandem Tilt-Wing eVTOL

The proposed control approach for generic transformational eVTOLs is analyzed and validated by applying the design to a tandem tilt-wing configuration. We use the configuration from previous works [10, 11, 14, 16].

A. Flight Dynamics Model

In order to apply the developed control approach, the flight dynamics model of the tandem tilt-wing aircraft described in [11] is used. The configuration has 14 control inputs, including eight propeller speed commands n_i, two tilt angle commands $\delta_{\mathrm{w},i}$, and four elevon control surface deflections (one per half-wing) $\delta_{\mathrm{e},i}$. They allow direct control over $\boldsymbol{m}_p^B$, the x- and z-component of $\boldsymbol{f}_{\mathrm{p}}^B$, as well $\boldsymbol{m}_{\mathrm{a}}^B$ and indirectly $\boldsymbol{f}_{\mathrm{a}}^B$.

However, since the high-fidelity flight dynamics model from [11] is rather complex, a surrogate model for inversion and control allocation is used. The reduced model uses strip theory following the formulation in [11, 17] but divides each half wing into only two *strips*. One strip is located mainly in the slipstream of the inner propeller, while the other is primarily in the slipstream of the outer propeller. This approach effectively accounts for the dominant effects of the tilt-wing dynamics. However, effects such as lift distribution, propeller swirl, or interactions between the tandem wings are neglected. Yet the comparison between both models shown in Fig. 2 suggests that the longitudinal forces and moments match sufficiently. Even the pitch moment still meets an acceptable level of quality, considering the significant gain in simplicity and performance through the model reduction.

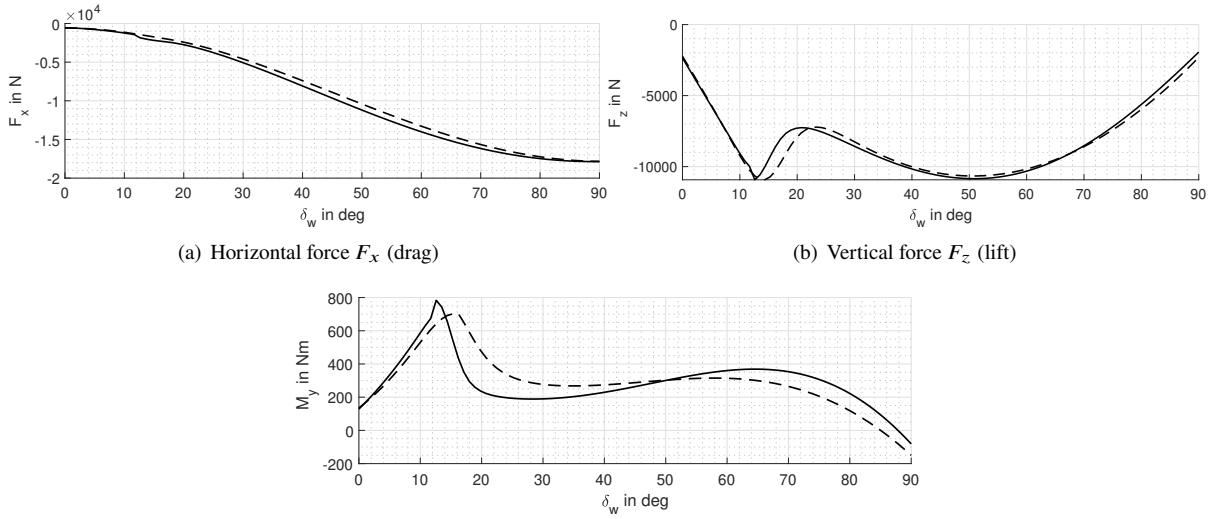

(a) Horizontal force F_x (drag)

(b) Vertical force F_z (lift)

(c) Pitch moment M_y

Fig. 2 Comparison of the longitudinal forces and moments along the tilt angle at an airspeed of $50\,\mathrm{m\,s^{-1}}$ between the high fidelity model from [11] (——) and the reduced model (- - -).

B. Model Analysis

Detailed studies of this (type of) aircraft have already been presented in [10, 11, 14, 18, 43]. Tilt-wings have the property that allows allocating propulsive forces in a two-dimensional space through the tilt angle $\delta_{\mathrm{w},i}$ and the propeller thrust T_j as

$$\boldsymbol{f}_{\mathrm{p}}^B = \sum_{i,j} \begin{bmatrix} \cos\delta_{\mathrm{w},i} \\ 0 \\ \sin\delta_{\mathrm{w},i} \end{bmatrix} T_j \tag{30}$$

which allows the inversion of $\boldsymbol{v}_{\mathrm{x}}^B$ and $\boldsymbol{v}_{\mathrm{z}}^B$. However, due to the dynamics of the tilt mechanism, the axes cannot be controlled completely independently. A more detailed analysis of this is given in [30] where the authors also propose a control scheme for $\boldsymbol{v}^E$. The authors implicitly assume a given tilt angle and use the thrust and inner-loop attitude controller to track a $\boldsymbol{v}^E$-command. This approach is clever, but it does not use the full potential of tilting wings. Despite

exerting a strong impact on the angle of attack and the flight path angle in the short term, the tilt angle eventually leads to a new trim velocity, approximately restoring the original flight path angle. In contrast, a change in thrust affects the velocity of the flight path in the short term, while influencing the flight path angle in the long term. This can easily be shown through simplified force-based flight path equations of a til wing. Assume a 2 DoF point-mass with a tilt (or thrust) angle δ_w, an angle of attack α causing aerodynamic drag D and lift L, flight path velocity V^K, and flight path angle γ. Then, the equilibrium flight is approximated by

$$T \cos\iota = D + m\,g \sin\gamma \tag{31}$$

$$T \sin\iota + L = m\,g \cos\gamma \tag{32}$$

with the incline $\iota = \alpha + \delta_\mathrm{w}$, which also represents the effective angle of attack determining the aerodynamic coefficients. The equations allow us to analyze the influence of a change in δ_w and T on the equilibrium flight path velocity and angle. Figure 3 shows how the equilibrium flight path velocity and angle change with increasing tilt angle and thrust. This motivates a control approach where the (commanded) velocity slowly changes the tilt angle. The thrust, however,

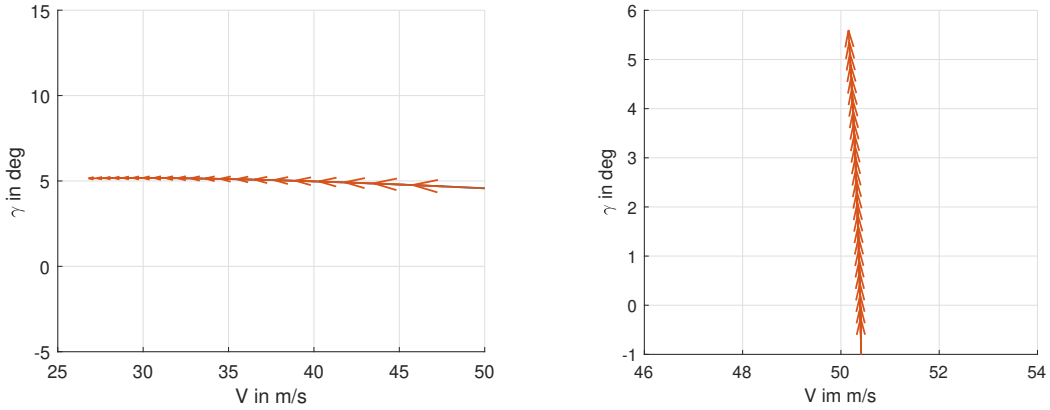

(a) Tilt angle δ_w (b) Thrust T

Fig. 3 Equilibrium flight path velocity V^K and flight path angle γ over different thrust T and tilt angle δ_w values. T increases along the arrows from 0 N to 500 N, and δ_w from 0° to 12°.

is used best for a (short-term) velocity change, but also a long-term flight path angle change. Nonetheless, due to the high bandwidth of electric propulsion systems, the (differential) thrust is used to control the commanded attitude and velocities, whereas the slow tilt actuators are used to adapt to the newly commanded trim state. This additionally motivates the use of a flight-path-centered description for the inversion. In the same way, differential tilt (combined with some differential thrust) can be utilized to achieve a pitch moment equilibrium in the long term. See [14] for more details on the pitch moment equilibrium.

C. Flight Control Design

The tilt-wing model and the generic transformational eVTOL system, as described in (6), differ in that the control inputs cannot directly control the side force. Consequently, (13) has rank 5, and thus, the inversion needs to be reduced to a 5-dimensional problem by canceling the side force component. Furthermore, the cost function for the allocation is defined as

$$L(\boldsymbol{x}, \boldsymbol{u}) = \frac{1}{2} (\boldsymbol{u} - \boldsymbol{u}_0)^T \boldsymbol{W} (\boldsymbol{u} - \boldsymbol{u}_0) \tag{33}$$

with the weight matrix $\boldsymbol{W}$ chosen according to common practice as the inverse of the maximum rates of the normalized input, as

$$\boldsymbol{W} = \mathrm{diag}\left(\begin{bmatrix} \frac{\dot{n}_\mathrm{max}^{-1}}{n_\mathrm{max}^2} & \dots & \frac{\dot{n}_\mathrm{max}^{-1}}{n_\mathrm{max}^2} & \frac{\dot{\delta}_{\mathrm{w,max}}^{-1}}{\delta_{\mathrm{w,max}}^2} & \frac{\dot{\delta}_{\mathrm{w,max}}^{-1}}{\delta_{\mathrm{w,max}}^2} & \frac{\dot{\delta}_{\mathrm{e,max}}^{-1}}{\delta_{\mathrm{e,max}}^2} & \dots & \frac{\dot{\delta}_{\mathrm{e,max}}^{-1}}{\delta_{\mathrm{e,max}}^2} \end{bmatrix}\right) \tag{34}$$

for the control input vector $\boldsymbol{u} = \begin{bmatrix} n_1 & \dots & n_8 & \delta_{\mathrm{w},1} & \delta_{\mathrm{w},2} & \delta_{\mathrm{e},1} & \dots & \delta_{\mathrm{e},4} \end{bmatrix}^T$. The pseudo control input vector $\boldsymbol{\nu}$ is consequently 5-dimensional and represents the angular accelerations $\dot{\boldsymbol{\omega}}^B$, and the accelerations in horizontal and

vertical direction $\dot{\boldsymbol{v}}_x^B$ and $\dot{\boldsymbol{v}}_z^B$, in the following denoted as $\boldsymbol{\nu} = \begin{bmatrix} \nu_p & \nu_q & \nu_r & \nu_u & \nu_w \end{bmatrix}^T$ where the common notation $\boldsymbol{\omega}^B = \begin{bmatrix} p & q & r \end{bmatrix}^T$ and $\boldsymbol{v}^B = \begin{bmatrix} u & v & w \end{bmatrix}^T$ is used. The pseudo control input vector is calculated from a linear compensator in a PID-like structure and follows

$$\begin{bmatrix} \nu_p \\ \nu_q \end{bmatrix} = \mathbb{T}_{B\Phi} \cdot \left(\left(\frac{K_i}{s} + K_p \right) \left(\begin{bmatrix} \phi_d \\ \theta_d \end{bmatrix} - \begin{bmatrix} \hat{\phi} \\ \hat{\theta} \end{bmatrix} \right) + K_d \left(\begin{bmatrix} \dot{\phi}_d \\ \dot{\theta}_d \end{bmatrix} - \begin{bmatrix} \hat{\dot{\phi}} \\ \hat{\dot{\theta}} \end{bmatrix} \right) + K_{ff} \begin{bmatrix} \ddot{\phi}_d \\ \ddot{\theta}_d \end{bmatrix} \right) \tag{35}$$

$$\nu_r = \left(\frac{K_i}{s} + K_p \right) (r_d - \hat{r}) \tag{36}$$

$$\begin{bmatrix} \nu_u \\ \nu_w \end{bmatrix} = \left(\frac{K_i}{s} + K_p \right) \left(\begin{bmatrix} u_d \\ w_d \end{bmatrix} - \begin{bmatrix} \hat{u} \\ \hat{w} \end{bmatrix} \right) \tag{37}$$

where $_d$ denotes desired quantities, $\hat{}$ measures ones, and $\mathbb{T}_{B\Phi}$ the kinematic inversion from Euler angle accelerations to body angular accelerations. A more detailed discussion of the control design can be found e.g. in the previous work [10].

D. Flight Controller Analysis

The developed control concept is novel, particularly regarding the combination of dynamic inversion, control allocation, and the eVTOL configuration. Therefore, it is first tested from the core, where the tracking performance is determined. Thus, we command different virtual control inputs on each axis and investigate the resulting accelerations. This way, we can investigate the accuracy of the combined inversion and control allocation but also investigate the physical limitations of the system.

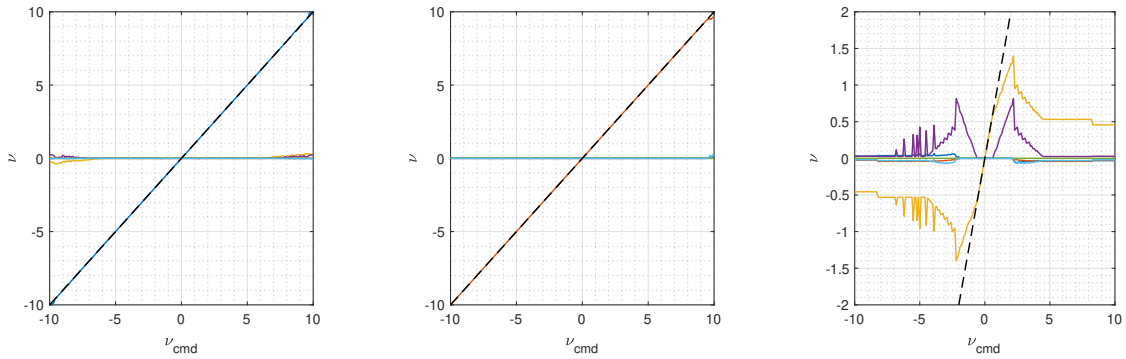

(a) Roll axis ν_p (b) Pitch axis ν_q (c) Yaw axis ν_r

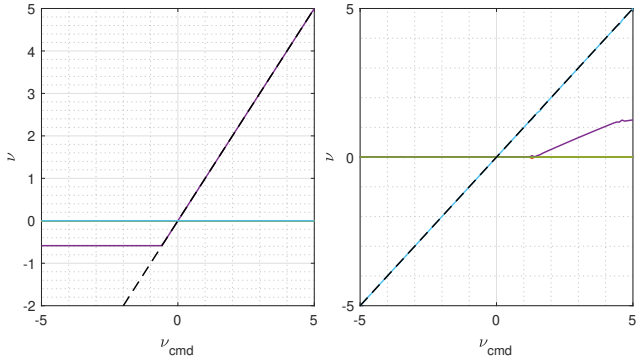

(d) Horizontal acceleration ν_u (e) Vertical acceleration ν_w

Fig. 4 The effect of the virtual control input in a single axis (- - -), computed via an iterative non-linear solver: Roll acceleration $\dot{p}$ (—), pitch acceleration $\dot{q}$ (—), yaw acceleration $\dot{r}$ (—), horizontal acceleration $\dot{u}$ (—), lateral acceleration $\dot{v}$ (—), and vertical acceleration $\dot{w}$ (—).

Figure 4 shows the results of this experiment using a perfect inversion and control allocation, i.e., a non-linear iterative solver solves (28a). This way, the physical limitations of the system, in combination with the general limitations of the approach, can be investigated. Subsequently, the proposed linear inversion and allocation are tested and compared. Figure 4(a) shows an almost perfect tracking of ν_p in a wide range. However, starting from (high) angular accelerations of $\pm 7\,\mathrm{rad\,s^{-2}}$, a slight coupling with other axes can be seen. This region is, however, outside the nominal operation conditions. Likewise, Fig. 4(b) suggests a perfect tracking of ν_q in a wide range. In contrast, the yaw axis shows a strong coupling and degradation of the tracking performance outside a narrow range of $-0.7\,\mathrm{rad\,s^{-2}}$ to $0.7\,\mathrm{rad\,s^{-2}}$. As Fig. 4(d) suggests, perfect tracking can be achieved for the (horizontal) acceleration. However, deceleration is limited to about $-0.7\,\mathrm{m\,s^{-2}}$. In addition, similar behavior can be observed for the vertical acceleration. In fact, climbing (i.e., acceleration in the negative z-direction) is possible in a large range and solely limited by the maximum motor power. However, a decrease is only possible until $1.2\,\mathrm{m\,s^{-2}}$ without simultaneous acceleration. From that point forward, only a decrease combined with an acceleration is feasible.

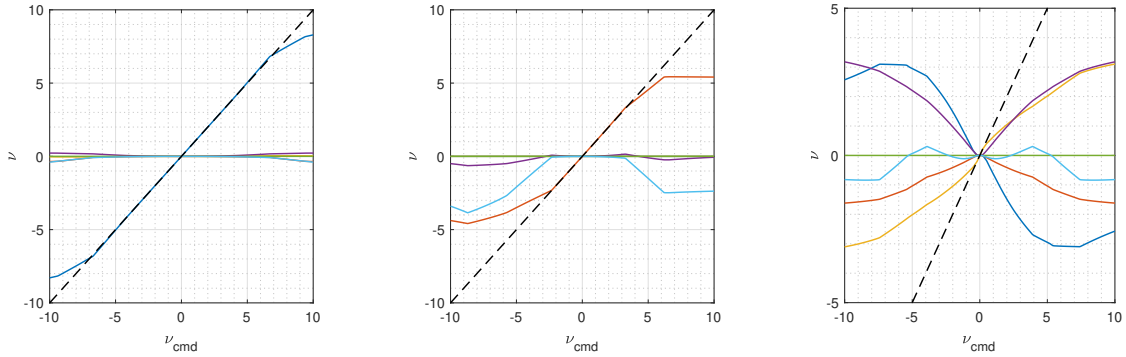

(a) Roll axis command ν_p (b) Pitch axis command ν_q (c) Yaw axis command ν_r

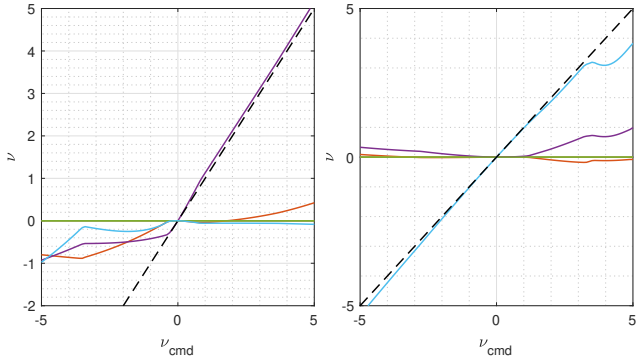

(d) Horizontal acceleration ν_u (e) Vertical acceleration ν_w

Fig. 5 The effect of the virtual control input in a single axis (- - -), computed via the linear control allocation: Roll acceleration $\dot{p}$ (——), pitch acceleration $\dot{q}$ (——), yaw acceleration $\dot{r}$ (——), horizontal acceleration $\dot{u}$ (——), lateral acceleration $\dot{v}$ (——), and vertical acceleration $\dot{w}$ (——).

Figure 5 depicts the same plots but for the linear control allocation strategy according to (25). While Fig. 5(a) shows comparable performance to Fig. 4(a), the pitch performance is more limited. Acceptable tracking performance without cross-couplings is only possible from $-2.5\,\mathrm{rad\,s^{-2}}$ to $3\,\mathrm{rad\,s^{-2}}$. The performance degradation is even more noticeable in Fig. 5(c). Only a narrow range from $-0.2\,\mathrm{rad\,s^{-2}}$ to $0.2\,\mathrm{rad\,s^{-2}}$ exhibits acceptable results. Tracking a horizontal acceleration command is limited with the linear control strategy to a range from $-0.3\,\mathrm{m\,s^{-2}}$ to $2\,\mathrm{m\,s^{-2}}$. Beyond this range, the acceleration either saturates or diverges from the command while inducing cross-couplings. Likewise, the vertical acceleration shows acceptable results in a range from $-1\,\mathrm{m\,s^{-2}}$ to $1\,\mathrm{m\,s^{-2}}$.

V. Discussion

This paper presents a holistic approach for solving the control problem of transformational eVTOLs, applied to a tandem tilt-wing configuration in Section IV. The results from Section IV are used to conclude the overall concept.

One major challenge with this approach is the complexity involved in calculating the pseudo-inverse $\boldsymbol{B}^{+}$ for (25), but also $\boldsymbol{\tau}$, which requires multiple evaluations of the (partial) flight dynamics model, particularly the function $\boldsymbol{g}(\boldsymbol{x}, \boldsymbol{u})$. Especially eVTOLs require elaborate models to account for their aerodynamic effects. Therefore, Section IV.A introduces a considerably reduced model of the present tilt-wing. Figure 2 compares the forces and moments across the full range of tilt angles and indicates that the reduced model adequately matches the high-fidelity one despite simplifications. As a result, the necessary foundation to execute the control system with higher sample rates is established.

Control approaches for eVTOLs differ from those for fixed-wing aircraft due to distinct dynamic effects that govern them. Fixed-wing aircraft are particularly centered around the attitude controller, meaning manual and flight path control is done in terms of attitude commands. A change in altitude is solely possible by a change in flight path angle. However, transformational eVTOLs typically alter their behavior during various flight phases and often offer several ways to change their flight state. For instance, tilt wings allow flight path control by adjusting their tilt angle and thrust, leading to the conceptualization of the flight control system as concluded in Section IV.B. Specifically, this motivates in selecting the design option to adjust the tilt angle command based on the current velocity and velocity command.

Section IV.D examines the results of the controller implementation according to Section IV.C. This work is an early step toward a generic transformational eVTOL control strategy and a tandem tilt-wing control law. Accordingly, the analysis concentrates on the controller's core, including the dynamic inversion and control allocation, which realize commanded accelerations from the velocity and attitude controllers. Figures 4 and 5 visualize the extent to which the control law effectively realizes commanded accelerations and decouples them from other motions.

Figure 4 depicts the effects and performance of the optimal allocation and inversion. While Fig. 4 suggests that no perfect decoupling of the axes is possible, it also suggests that this is not owed to the control approach but the eVTOL configuration's physical limitations. The roll and pitch axis are almost entirely decoupled and controllable. The performance of the pitch axis control is reinforced by the characteristics of tilt-wings that allow them to uncouple the angle of attack α and pitch angle θ with the help of the tilt angles. In contrast, the yaw axis has a limited envelope and readily cross-couples with the forward acceleration $\dot{u}$. This can be explained physically: A yaw moment necessitates differential thrust, which is restricted here since the low thrust setting at cruise equilibrium limits the ability to reduce thrust on one side. Thus, the overall thrust must be raised to increase the yaw moment, resulting in forward acceleration. However, this limitation does not restrict the flight performance since the main purpose of ν_r is regulating the angle of sideslip β. The results on the tracking performance of the translational accelerations show behavior similar to other publications on tilt-wings, mainly because deceleration is limited for these types of vehicles: Both translational axes suffer from the deceleration problem of tandem tilt-wings [10–12]. Acceleration in the forward direction is feasible within a large range due to the excess power of the propulsion, while deceleration is severely restricted. A similar trend can be seen for the vertical acceleration: While ascending can take place over a broader range, decreasing swiftly results in a forward acceleration of the vehicle. These effects have to be considered in the calculation of ν_u and ν_w since there is an inherent physical coupling. However, these results are achieved through a costly iterative optimization process and are inadequate for closed-loop systems with real-time requirements.

On these grounds, Fig. 5 illustrates the same properties but for the linear control allocation (25). As anticipated, reducing computational costs leads to less accurate tracking. Consequently, parasitic coupling can be observed especially far from the expansion point. This originates mainly from the dynamic inversion tracking constraint being reduced to its first-order Taylor series approximation. Thus, the solution only holds within the neighborhood of a freely specified $\boldsymbol{u}_0$, commonly chosen as the current control command $\hat{\boldsymbol{u}}$. Although many publications do not distinguish between $\boldsymbol{u}_0$ and $\hat{\boldsymbol{u}}$, this work's formulation intentionally separates the two because $\boldsymbol{u}_0$ can be adjusted to improve the accuracy of linear control allocation. In fact, Fig. 5 demonstrates acceptable tracking performance within a specific range around $\boldsymbol{u}_0$, which was chosen as the zero point. While the roll acceleration is effectively decoupled and tracked over a large range, the envelope for the pitch axis is narrower but still reasonable. Meanwhile, the already physically limited yaw envelope is further reduced. However, this channel is solely employed to stabilize the angle of sideslip during cruise flight and not for agile maneuvers. Thus, even a narrow margin is sufficient for the intended application. The same applies to the translational accelerations. Although the commands diverge and parasitic accelerations fade in for commands far from the expansion point, reasonable tracking performance is still achievable within a restricted acceleration range, which appears to satisfy the planned application.

Consequently, while the control design has not undergone full closed-loop control validations, the findings suggest a reasonable design for the present tandem tilt-wing configuration.

VI. Conclusion

In this study, a generic representation for transformational eVTOLs is sought and proposed, along with a dynamic inversion-based control and control allocation approach. Moreover, this approach is applied to a tandem tilt-wing configuration. The existing high-fidelity model is reduced to a surrogate model to improve the efficiency of the controller implementation. Reducing the complexity of the model also aids in gathering relevant physical insights for control design. Initial results utilizing this control approach show promising outcomes. When using the costly nonlinear control allocation, solely physical limitations of the vehicle degrade the performance. In contrast, while the proposed linear control approach shows similar performance in the neighborhood of the expansion point, commands outside exhibit poor performance and strong cross-couplings. This is, however, expected due to the nature of the Taylor series expansion. Thus, we can continue to explore the proposed approach in future studies and delve into greater detail. Consecutive studies will focus on manual and mission flight performance exhibited by a full high-fidelity tilt-wing model.

References

[1] Anderson, S. B., "Historical Overview of V/STOL Aircraft Technology," Tech. rep., NASA, 1981. NASA/TM-1997-81280.

[2] Sullivan, T., "The Canadair CL-84 tilt wing design," *Aircraft Design, Systems, and Operations Meeting*, 1993. https://doi.org/10.2514/6.1993-3939.

[3] O'Brien, M. A., "The V-22 Osprey: A Case Analysis," Master's thesis, Naval Postgraduate School, 1992.

[4] Bacchini, A., and Cestino, E., "Electric VTOL Configurations Comparison," *Aerospace*, Vol. 6, No. 3, 2019. https://doi.org/10.3390/aerospace6030026.

[5] Chana, W. F., and Sullivan, T., "The Tilt Wing Configuration for High Speed VSTOL Aircraft," *ICAS 1994*, 1994.

[6] Lombaerts, T., Kaneshige, J., and Feary, M., "Control Concepts for Simplified Vehicle Operations of a Quadrotor eVTOL Vehicle," *AIAA Aviation 2020 Forum*, 2020.

[7] Al Haddad, C., Chaniotakis, M., Straubinger, A., Plötner, K., and Antoniou, C., "Factors affecting the adoption and use of urban air mobility," *Transportation Research Part A Policy and Practice*, Vol. 132, 2020, pp. Pages 696–712. https://doi.org/10.1016/j.tra.2019.12.020.

[8] Denham, J., and Paines, J., "Converging on a Precision Hover Control Strategy for the F-35B STOVL Aircraft," *AIAA Guidance, Navigation and Control Conference and Exhibit*, 2008. https://doi.org/10.2514/6.2008-6331.

[9] Nordeen, L., *Harrier II : validating V/STOL*, Naval Institute Press, Annapolis, Md, 2006.

[10] Milz, D., and Looye, G., "Tilt-Wing Control Design for a Unified Control Concept," *AIAA SCITECH 2022 Forum*, 2022. https://doi.org/10.2514/6.2022-1084.

[11] May, M., Milz, D., and Looye, G., "Semi-Empirical Aerodynamic Modeling Approach for Tandem Tilt-Wing eVTOL Control Design Applications," *AIAA SCITECH 2023 Forum*, 2023. https://doi.org/10.2514/6.2023-1529.

[12] May, M., Milz, D., and Looye, G., "Transition Strategies for Tilt-Wing Aircraft," *AIAA SCITECH 2024 Forum*, American Institute of Aeronautics and Astronautics, 2024.

[13] Menon, P. K. A., Badgett, M. E., Walker, R. A., and Duke, E. L., "Nonlinear flight test trajectory controllers for aircraft," *Journal of Guidance, Control, and Dynamics*, Vol. 10, No. 1, 1987, pp. 67–72. https://doi.org/10.2514/3.20182.

[14] Perdolt, D., Milz, D., May, M. S., and Thiele, M., "Efficient Mid-Fidelity Aerodynamic Modeling of a Tilt-Wing eVTOL for Control Applications," *33rd Congress of the International Council of the Aeronautical Sciences, ICAS 2022*, 2022.

[15] Montagnani, D., Tugnoli, M., Zanotti, A., Syal, M., and Droandi, G., "Analysis of the Interactional Aerodynamics of the Vahana eVTOL Using a Medium Fidelity Open Source Tool," *VFS Aeromechanics for Advanced Vertical Flight Technical Meeting*, 2020.

[16] May, M., Milz, D., and Looye, G., "Dynamic Modeling and Analysis of Tilt-Wing Electric Vertical Take-Off and Landing Vehicles," *AIAA 2022 Scitech Forum*, 2022.

[17] Cook, J., "A Strip Theory Approach to Dynamic Modeling of eVTOL Aircraft," *AIAA Scitech 2021 Forum*, 2021. https://doi.org/10.2514/6.2021-1720.

[18] Panish, L., and Bacic, M., "Transition Trajectory Optimization for a Tiltwing VTOL Aircraft with Leading-Edge Fluid Injection Active Flow Control," *AIAA SCITECH 2022 Forum*, 2022. https://doi.org/10.2514/6.2022-1082.

[19] Panish, L., Nicholls, C., and Bacic, M., "Nonlinear Dynamic Inversion Flight Control of a Tiltwing VTOL Aircraft," *AIAA SCITECH 2023 Forum*, American Institute of Aeronautics and Astronautics, 2023. https://doi.org/10.2514/6.2023-1910.

[20] Simmons, B. M., and Murphy, P. C., "Wind Tunnel-Based Aerodynamic Model Identification for a Tilt-Wing, Distributed Electric Propulsion Aircraft," *AIAA Scitech 2021 Forum*, 2021. https://doi.org/10.2514/6.2021-1298.

[21] Simmons, B. M., and Murphy, P. C., "Aero-Propulsive Modeling for Tilt-Wing, Distributed Propulsion Aircraft Using Wind Tunnel Data," *Journal of Aircraft*, Vol. 59, No. 5, 2022, pp. 1162–1178. https://doi.org/10.2514/1.C036351.

[22] Lombaerts, T., Kaneshige, J., Schuet, S., Hardy, G., Aponso, B. L., and Shish, K. H., "Nonlinear Dynamic Inversion Based Attitude Control for a hovering quad tiltrotor eVTOL vehicle," *AIAA Scitech 2019 Forum*, 2019. https://doi.org/10.2514/6.2019-0134.

[23] Di Francesco, G., and Mattei, M., "Modeling and Incremental Nonlinear Dynamic Inversion Control of a Novel Unmanned Tiltrotor," *Journal of Aircraft*, Vol. 53, No. 1, 2016, pp. 73–86. https://doi.org/10.2514/1.C033183.

[24] Yanguo, S., and Huanjin, W., "Design of Flight Control System for a Small Unmanned Tilt Rotor Aircraft," *Chinese Journal of Aeronautics*, Vol. 22, No. 3, 2009, pp. 250–256. https://doi.org/10.1016/S1000-9361(08)60095-3.

[25] Hartmann, P., Schütt, M., and Moormann, D., "Konzept eines stetigen Bahnreglers für den vollständigen Flugbereich eines Kippflügelflugzeuges," *Publikationen zum DLRK 2014 : 63. Deutscher Luft- und Raumfahrtkongress 2014*, edited by DGLR, 2014.

[26] Hartmann, P., Meyer, C., and Moormann, D., "Unified Velocity Control and Flight State Transition of Unmanned Tilt-Wing Aircraft," *Journal of Guidance, Control, and Dynamics*, Vol. 40, No. 6, 2017, pp. 1348–1359. https://doi.org/10.2514/1.g002168.

[27] Cetinsoy, E., Dikyar, S., Hancer, C., Oner, K. T., Sirimoglu, E., Unel, M., and Aksit, M. F., "Design and construction of a novel quad tilt-wing UAV," *Mechatronics*, Vol. 22, No. 6, 2012, pp. 723–745. https://doi.org/10.1016/j.mechatronics.2012.03.003.

[28] Öner, K. T., Çetinsoy, E., Sirimoğlu, E., Hançer, C., Ünel, M., Akşit, M. F., Gülez, K., and Kandemir, I., "Mathematical modeling and vertical flight control of a tilt-wing UAV," *Turkish Journal of Electrical Engineering & Computer Sciences*, Vol. 20, No. 1, 2012, pp. 149–157.

[29] Raab, S. A., Zhang, J., Bhardwaj, P., and Holzapfel, F., "Proposal of a Unified Control Strategy for Vertical Take-off and Landing Transition Aircraft Configurations," *2018 Applied Aerodynamics Conference*, American Institute of Aeronautics and Astronautics, 2018. https://doi.org/10.2514/6.2018-3478.

[30] Panish, L., and Bacic, M., "A Generalized Full-Envelope Outer-Loop Feedback Linearization Control Strategy for Transition VTOL Aircraft," *AIAA AVIATION 2023 Forum*, American Institute of Aeronautics and Astronautics, 2023. https://doi.org/10.2514/6.2023-4511.

[31] Axten, R. M., Khamvilai, T., and Johnson, E. N., "VTOL Freewing Design and Adaptive Controller Development," *AIAA SCITECH 2023 Forum*, 2023. https://doi.org/10.2514/6.2023-0401.

[32] Surmann, D., and Myschik, S., "Gain Design of an INDI-based Controller for a Conceptual eVTOL in a Nonlinear Simulation Environment," *AIAA SCITECH 2023 Forum*, 2023. https://doi.org/10.2514/6.2023-1250.

[33] Lombaerts, T., Kaneshige, J., Schuet, S., Aponso, B. L., Shish, K. H., and Hardy, G., "Dynamic Inversion based Full Envelope Flight Control for an eVTOL Vehicle using a Unified Framework," *AIAA Scitech 2020 Forum*, 2020. https://doi.org/10.2514/6.2020-1619.

[34] Pollack, T., and Kampen, E.-J. V., "Multi-objective Design and Performance Analysis of Incremental Control Allocation-based Flight Control Laws," *AIAA SCITECH 2023 Forum*, 2023. https://doi.org/10.2514/6.2023-1249.

[35] Lombaerts, T., and Looye, G., "Design and Flight Testing of Nonlinear Autoflight Control Laws," *AIAA Guidance, Navigation, and Control Conference 2012*, 2012. https://doi.org/10.2514/6.2012-4982.

[36] Holzapfel, F., "Nichtlineare adaptive Regelung eines unbemannten Fluggerätes," Ph.D. thesis, Technischen Universität München, 2004.

[37] Enns, D., Bugajski, D., Hendrick, R., and Stein, G., "Dynamic inversion: an evolving methodology for flight control design," *International Journal of Control*, Vol. 59, No. 1, 1994, pp. 71–91. https://doi.org/10.1080/00207179408923070.

[38] Milz, D., Looye, G., and May, M., "Dynamic Inversion: An Incrementally Evolving Methodology for Flight Control Design," 2024. To be published.

[39] Smith, P., "A simplified approach to nonlinear dynamic inversion based flight control," *23rd Atmospheric Flight Mechanics Conference*, American Institute of Aeronautics and Astronautics, 1998. https://doi.org/10.2514/6.1998-4461.

[40] Pfeifele, O., and Fichter, W., "Energy Optimal Control Allocation for INDI Controlled Transition Aircraft," *AIAA Scitech 2021 Forum*, 2021. https://doi.org/10.2514/6.2021-1457.

[41] Durham, W., *Aircraft control allocation*, Aerospace series, Wiley, Chichester, West Sussex, United Kingdom, 2017. Includes bibliographical references (pages 247-275) and index.

[42] Johansen, T. A., and Fossen, T. I., "Control allocation—A survey," *Automatica*, Vol. 49, No. 5, 2013, pp. 1087–1103. https://doi.org/10.1016/j.automatica.2013.01.035.

[43] Cook, J., "Exploration of Dynamic Transitions of Tiltwing Aircraftusing Differential Geometry," Ph.D. thesis, University of Colorado, 2022.